Clim. Past Discuss., 6, 2557–2591, 2010
www.clim-past-discuss.net/6/2557/2010/
doi:10.5194/cpd-6-2557-2010

Climate of the Past Discussions

Glacial cycles and solar insolation: the role of orbital, seasonal, and spatial variations

R. K. Kaufmann[1] **and K. Juselius**[2]

[1]Boston University, Boston, USA
[2]University of Copenhagen, Copenhagen, Denmark

Received: 13 October 2010 – Accepted: 18 October 2010 – Published: 16 November 2010

Correspondence to: R. K. Kaufmann (kaufmann@bu.edu)

Published by Copernicus Publications on behalf of the European Geosciences Union.

Abstract

We use a statistical model, the cointegrated vector autoregressive model, to evaluate the relative roles that orbital, seasonal, and spatial variations in solar insolation play in glacial cycles during the late Quaternary (390kyr – present). To do so, we estimate models of varying complexity and compare the accuracy of their in-sample simulations. Results indicate that variations in solar insolation associated with changes in Earth's orbit have the greatest explanatory power and that obliquity, precession, and eccentricity are needed to generate an accurate simulation of glacial cycles. Seasonal variations in insolation play a lesser role, while cumulative summer-time insolation has little explanatory power. Finally, solar insolation in the Northern Hemisphere generates the more accurate in-sample simulation of surface temperature while ice volume is simulated most accurately by solar insolation in the Southern Hemisphere.

1 Introduction

According to Paillard (2001), Adhemar (1842) is among the first to link changes in climate to variations in Earth's orbit, specifically precessional changes in the equinox. Croll (1875) formalizes this notion by postulating that seasonal changes in solar insolation, which are associated with precession, cause ice sheets to grow and shrink. This explanation is expanded to include changes in eccentricity, precession, and obliquity by Milankovitch (1941). His model hypothesizes that glacial cycles coincide with the 23 and 41 kyr periods of precession and obliquity. This hypothesis is confirmed by Hays et al. (1976) who examine the periodicity of ice sheets. Since then, the main features of "the Milankovitch theory" have been confirmed many times.

Despite these successes, not all aspects of glacial cycles can be explained by the Milankovitch theory. Among the most notable is the so-called "100 kyr problem." Reconstructions of ice volume based on δ^{18}O indicate that the accumulation and ablation of ice sheets show a very strong 100 kyr cycle during the late Pleistocene (Schackleton

CPD
6, 2557–2591, 2010

R. K. Kaufmann and K. Juselius

and Opdyke, 1973). This periodicity is problematic for theories that stress orbital cycles (Imbrie et al., 1993) because the amplitude of the insolation signal associated with eccentricity is only about 2 W/m^2. This change is much smaller than the change associated with precession (~100 W/m^2) and obliquity (~20 W/m^2) and is the heart of the 100 kyr problem – why does the climate system respond so strongly to small changes in solar insolation that are associated with eccentricity?

Efforts to answer this question in particular, and to better understand glacial cycles in general, take two approaches. One approach seeks to identify mechanisms that connect ice-volumes to other climate variables. Mechanisms include changes in the atmospheric concentrations of carbon dioxide (Saltzman and Maasch, 1990) and interplanetary dust particles (Muller and MacDonald, 1997). To evaluate these hypotheses, analysts often use statistical techniques (either ordinary least squares or spectral techniques) to link a proxy for the mechanism of interest with either temperature and/or ice volume. For example, there is a close and seemingly stable correlation between atmospheric CO_2 and temperature (Paillard, 2001; Siegenthaler et al., 2005; Martinez-Garcia et al., 2009; Luthe et al., 2008), CO_2 and ice volume (Martinez-Garcia et al., 2009), CO_2 and dust (Bender, 2003), and sodium and temperature (Petit et al., 1999; Wolff et al., 2006). Some of these correlations are strong, as measured by diagnostic statistics. For example, the linear relationship between CO_2 and Antarctic temperature during the previous 800 kyr has an R^2 (also known as the adjusted coefficient of determination) of 0.82, which indicates that 82% of the variation in Antarctic temperature is associated with variation in atmospheric CO_2 (Luthe et al., 2008). Similarly, Shackleton (2000) finds that deep water temperature is highly coherent (0.97) with the Vostok CO_2 signal. Despite the obvious relationships among variables, the direction of cause-and-effect among climate variables is uncertain.

A second approach, which is not mutually exclusive, is to identify the season(s) when and the latitude(s) where changes in solar insolation have the greatest effect on glacial cycles. This approach examines measures of solar insolation that go beyond eccentricity, precession, and obliquity because the complexity of the full Milkankovitch cycle

CPD
6, 2557–2591, 2010

implies that the system responds to insolation at many different places and seasons (Imbrie et al., 1993). Several studies highlight the importance of solar insolation in the Northern Hemisphere (Hays, 1978; Lorius et al., 1999; Raymo, 1997; Imbrie et al., 1993; Petit et al., 1999; Masson et al., 2000; Jouzel et al., 2007; Kawamura et al., 2007). For example, Kawamura et al. (2007) argue that "southern solar insolation is in antiphase or is completely out of phase, with Antarctic climate . . . these phasings suggest that Antarctic climate is paced by northern summer insolation presumably through northern ice sheet variation." But the importance of Northern Hemisphere insolation is disputed by others. Huybers and Denton (2008) argue that insolation during the Southern Hemisphere summer is the more important driver of temperature in the Antarctic.

In this paper, we evaluate the roles that orbital, seasonal, and spatial variations in solar insolation play in glacial cycles during the late Quaternary period (391 kyr – present) using a recent statistical modelling tool – the cointegrated vector autoregressive (CVAR) model. It represents a general methodology that maintains the assumption that the mechanisms which generate glacial cycles are highly complex and characterized by strong dynamics and simultaneous feed-back effects. This contrasts with single equation multiple regression models that postulate a causal mechanism a priori and disregard feedback effects. If climate mechanisms are inherently simultaneous, multidimensional, and dynamic, then results from such a single equation model can be (and often are) misleading.

To assess the role of exogenous drivers for glacial cycles, we estimate models of varying complexity and compare the accuracy of their in-sample simulations. Results indicate that variations in solar insolation associated with changes in Earth's orbit have the greatest explanatory power and that obliquity, precession, and eccentricity are needed to generate an accurate simulation of glacial cycles. Seasonal variations in insolation play a lesser role, while cumulative summer-time insolation has little explanatory power. Finally, solar insolation in the Northern Hemisphere generates a more accurate in-sample simulation of surface temperature, ice volume is simulated most accurately by solar insolation in the Southern Hemisphere, while the accuracy of the in-sample simulation for atmospheric CO_2 is relatively unaffected by latitutdinal measures of solar insolation.

These results and the methods used to obtain them are described in four sections. Section 2 describes the data and the statistical techniques that are used to estimate and compare the statistical models. Results are described in Sect. 3. Section 4 discusses how these results can be used to test various hypotheses about the roles that orbital, seasonal, and spatial variations in solar insolation play in glacial cycles. Section 5 concludes by describing how future efforts will build on this statistical approach to estimate temperature sensitivity, test hypotheses about climate dynamics, and test the hypothesis that human activity had a significant effect on climate well before the start of the industrial revolution.

2 Data and statistical methodology

2.1 Data

The late Quaternary "Vostok" period contains four "glacial cycles" and our empirical focus on this period reduces data aggregation across cores. We assemble data on three measures of glacial cycles; land surface temperature (*Temp*), carbon dioxide (CO_2), and ice volume (*Ice*). Surface temperature, atmospheric CO_2, and ice volume are among the most commonly used proxies for glacial cycles and are thought to be directly related to one another, and so their inclusion requires little justification.

Data for surface temperature and carbon dioxide are obtained from cores drilled into the Antarctic ice sheet, and therefore represent local conditions. Carbon dioxide is a well-mixed gas and so measurements from the Antarctic ice sheet probably represents global levels. The temperature measure represents local conditions, but can be converted to global values (Masson-Delmotte et al., 2006, 2010). Data on ice volume are derived from 57 cores drilled by the Deep-Sea Drilling Project and Ocean Drilling Program across the globe.

CPD
6, 2557–2591, 2010

To make these data amenable to a statistical analysis, we convert them to a common time scale (EDC3) using conversions from Parrenin et al. (2007) and Ruddiman and Raymo (2003). Unevenly spaced observations are interpolated (linearly) to generate a data set in which each time series has a time step of 1 kyr. Sources for these data, the number of observations, units of measure, and their original time scale are given in Table 1.

Solar insolation is exogenous to the statistical models and this driver is represented using several time series. Changes in Earth's orbit are represented by times series for precession, obliquity, and eccentricity. These changes generate spatial and temporal variations that are represented by time series for the radiation received at a specific latitude (e.g. 65° N) on a given day (e.g. 21 June–Summer). We also represent the effect of summer-time insolation with cumulative insolation on days during which insolation exceeds a pre-defined threshold (Huybers and Denton, 2008). For example, *Insol275* is a time series for cumulative annual insolation for days on which daily insolation exceeds 27 W/m^2 at a specific latitude.

2.2 Statistical analysis of stationary versus nonstationary data: an introductory discussion

There are many ways to describe climate time series – here we focus on the difference between stationary and non-stationary time series. A stationary time series does not exhibit trending behavior whereas a nonstationary series does. Such trends can be either deterministic or stochastic, the difference being that the increments of a deterministic trend are constant over time whereas those of a stochastic trend are random. While both can appear in climate data, stochastic trends are more valuable because they offer a way of identifying the underlying causes of permanent shocks to the climate.

CPD
6, 2557–2591, 2010

A simple example of a variable containing a stochastic trend is given by the so called random walk model:

$$x_t = x_{t-1} + \varepsilon_t, \tag{1}$$

or

$$\Delta x_t = \varepsilon_t$$

where ε_t is an independently, identically, normally distributed random shock with variance σ_ε^2 and Δ is the first difference operator (e.g. $x_t - x_{t-1}$). An equivalent description of Eq. (1) is:

$$x_t = x_0 + \varepsilon_1 + \varepsilon_2 + \ldots + \varepsilon_t = \sum_{i=1}^{t} \varepsilon_i + x_0, \quad t = 1, \ldots t \tag{2}$$

showing that today's value of x_t (for example temperature) is the sum of all previous temperature shocks, ε, starting from an initial date x_0. This cumulation of random shocks, $\sum_{i=1}^{t} \varepsilon_i$, is called a stochastic trend.

The random walk model can be seen as a special case of the AR(1) model:

$$x_t = \rho\, x_{t-1} + \varepsilon_t \tag{3}$$

which can be written as:

$$x_t = \sum_{i=1}^{t} \rho^{t-i} \varepsilon_i + \rho^t x_0, \quad t = 1, \ldots t$$

which is stationary if $|\rho| < 1.0$. In this case the effect of the shock (for example due to an increase in CO_2), ε_t, on the temperature would die out over time. How long this takes depends on the size of ρ: the closer to 1.0 the longer it takes. At the other opposite, if $\rho = 0$, a shock would have no permanent effect on temperature.

The variance of an AR(1) process is

$$\mathrm{VAR}(x_t) = \sigma_\varepsilon^2/(1-\rho). \tag{4}$$

showing that the variance becomes very large when ρ is close to 1.0. If $\rho = 1$, then x_t is nonstationary and Eq. (4) becomes undefined. In this case the variance increases over time, i.e. $\mathrm{VAR}(x_t) = t\sigma_\varepsilon^2$ and the mean is zero, i.e. $E(x_t) = 0$. Because variance increases over time, it is not possible to predict when or if a random walk will cross its mean value: a nonstationary variable is not significantly mean reverting. This implies that the sample average $\bar{x}$ is a biased estimator of the mean and that the sum of squares $\sum(x-\overline{x})_t^2$ is not an appropriate measure of the variance of a nonstationary variable. In other words, $\overline{x}$ is a very poor "reference line" when x_t is a random walk (as evident from the graphs of *Temp*, CO_2, and *Ice* in Fig. 1a–c).

2.3 Why is it important to differentiate between stationary and nonstationary time series when doing OLS regressions?

The preceding discussion may cause the reader to wonder, why is this important? Consider the "best guess" one would make about the value of x at time $t+1$ given information about x up to time t. For a random walk, this is x_t, whereas for a stationary, non-trending time series the best guess would be the average value. Therefore, when the series is stationary and time independent the deviation from the average is a good measure of how much x_t has changed, whereas when x_t is nonstationary it is the deviation from the previous value that measures how much x_t has changed. In this case $\sum(x_t-\overline{x})^2 \gg \sum(x_t-x_{t-1})^2$.

This has implications both for how to calculate R^2 and for how to measure associations between variables. If a stationary time independent variable is regressed on another variable, R^2 would correctly measure how much more the regressor variable has been able to explain of the variation in the regressand compared to its mean value. If a nonstationary variable is regressed on another nonstatioanary variable, one would

CPD
6, 2557–2591, 2010
Glacial cycles: drivers
R. K. Kaufmann and K. Juselius

say that it has explanatory value only if it beats the random walk model. In this case R^2 should be calculated for a model defined for Δx_t rather than x_t.

If a nonstationary time series is analyzed statistically using ordinary least squares (OLS) methods designed for stationary time series, the results may easily suggest a relationship when none exists. This problem, already shown by Yule (1929), can be illustrated with the following simple example:

Consider two unrelated random walks:

$$\Delta x_{1,\mathrm{t}} = \varepsilon_{1,\mathrm{t}} \text{ where } \varepsilon_{1,\mathrm{t}} \sim \text{ IN } \left[0, \sigma^2_{\varepsilon_1}\right]$$

$$\Delta x_{2,\mathrm{t}} = \varepsilon_{2,\mathrm{t}} \text{ where } \varepsilon_{2,\mathrm{t}} \sim \text{ IN } \left[0, \sigma^2_{\varepsilon_2}\right]$$

where IN stands for independent normal and $\mathrm{Cov}(\varepsilon_{1,\mathrm{t}}, \varepsilon_{2,\mathrm{t}}) = 0$. Assume that the equation of interest is:

$$x_{1,\mathrm{t}} = \beta\, x_{2,\mathrm{t}} + u_t \tag{5}$$

Using OLS to estimate Eq. (5) implicitly assumes that u_t is a stationary, independent error term. In this case the t-statistic (as calculated by a standard regression package) for testing $H_0/\beta = 0$ would satisfy $P\left(\left|t_{\beta_1=0}\right| \geq 2.0\ H_0\right) = 0.05$. When $\beta = 0$ in Eq. (5), $u_t = \Sigma\ \varepsilon_{1,i}$ and, therefore u_t is nonstationary. Based on a Monte Carlo experiment Hendry and Juselius (2000) show that a critical value of 14.8 (rather than 2.0) defines the 5% rejection frequency under the null for $T = 100$. Clearly, using OLS to analyze the relationship between nonstationary variables would often lead us to mistakenly believe that there is a relationship between variables in Eq. (5) when no relationship exists. This is what Yule called a spurious relationship.

The condition that two nonstationary variables are truly related is that they share the same stochastic trend. Regressing $x_{1,\mathrm{t}}$ on $x_{2,\mathrm{t}}$ in this case will eliminate the stochastic trend rendering u_t stationary and $x_{1,\mathrm{t}}$ and $x_{2,\mathrm{t}}$ are said to be cointegrated. Thus a cointegrating relation, $x_{1,\mathrm{t}} - \beta x_{2,\mathrm{t}}$, can be stationary in spite of $x_{1,\mathrm{t}}$ and $x_{2,\mathrm{t}}$ both

CPD
6, 2557–2591, 2010

R. K. Kaufmann and K. Juselius

being nonstationary. This property is exploited and formalized by the Cointegrated VAR (CVAR) model.

2.4 Analysing relationships among nonstationary time series: the CVAR model

The Cointegrated VAR model builds on the above results: nonstationary variables (containing stochastic trends) can be made stationary by differencing the series and by taking certain linear combinations of the series. While differencing removes all long-run information in the data, cointegration ensures that it is preserved. Beyond generating reliable and precise results, the CVAR model is able to capture both the long run equilibrium relationships among time series for endogenous climate variables and exogenous solar insolation and the dynamics by which the endogenous variables move towards equilibrium. These general aspects of the CVAR model are described below – for a formal description of the statistical properties of the CVAR model, see Juselius (2006).

The CVAR model assume that all climate variables, x_t, are endogenously determined, whereas all solar variables, w_t, are exogenous. Maintaining this distinction, the CVAR model is defined by the following equation:

$$\Delta \boldsymbol{x}_t = \boldsymbol{\Gamma}_1 \Delta \boldsymbol{x}_{t-1} + \boldsymbol{\Pi} \left(\boldsymbol{x}'_{t-1}, \boldsymbol{w}'_{t-1} \right)' + A_0 \Delta \boldsymbol{w}_t + \mathbf{A}_1 \Delta \boldsymbol{w}_{t-1} + \boldsymbol{\mu} + \varepsilon_t \quad (6)$$

where $\boldsymbol{x}_t$ is a $p \times 1$ vector of variables whose behavior is being modeled endogenously (e.g. *Temp*, CO_2, and *Ice*), $\boldsymbol{w}_t$ is a $pw \times 1$ vector of exogenous solar variables (e.g. eccentricity, obliquity, and precession), $\boldsymbol{\Gamma}_1$, $\boldsymbol{\Pi}$, $\mathbf{A}_0$, $\mathbf{A}_1$ are matrices of regression coefficients, $\boldsymbol{\mu}$ is a $p \times 1$ vector of constant terms, and $\varepsilon_t \sim$Niid$(0,\Omega)$.

When the data are nonstationary, the long-run matrix $\boldsymbol{\Pi}$ is generally of reduced rank, r. This is formulated as:

$$\boldsymbol{\Pi} = \boldsymbol{\alpha} \boldsymbol{\beta}' \quad (7)$$

where $\boldsymbol{\alpha}$ is a $p \times r$ matrix of adjustment coefficients and $\boldsymbol{\beta}$ is $r \times p$ matrix of cointegration coefficients that define stationary deviations from long-run equilibrium

CPD
6, 2557–2591, 2010

Glacial cycles: drivers

R. K. Kaufmann and K. Juselius

relationships. If the stochastic trend movements in $\boldsymbol{x}_t$ are exclusively associated with the movements of the exogenous drivers, the $\mathbf{\Pi}$ matrix would be of full rank and each climate variable would be cointegrated with the exogenous drivers, i.e. $x_{i,\mathrm{t}} = f(\boldsymbol{w}_t) + u_{i,\mathrm{t}}$ where $u_{i,\mathrm{t}}$ is a stationary error term. If the exogenous solar variables are not sufficient to explain the stochastic trend movements in $\boldsymbol{x}_t$, then the $\mathbf{\Pi}$ matrix would be of reduced rank. This would imply that the internal climate dynamics generate additional stochastic trends that drive glacial cycles.

The CVAR model is designed to simulate why temperature changes from the previous period to the present based on lagged dynamic effects from previous changes in temperature, CO_2, and *Ice* ($\mathbf{\Gamma}_1 \Delta \boldsymbol{x}_{\mathrm{t}-1}$), current and lagged dynamic effect from changes in solar variables ($\mathbf{A}_0 \Delta \boldsymbol{w}_t \mathbf{A}_1 \Delta \boldsymbol{w}_{\mathrm{t}-1}$) and finally by the dynamic adjustment towards long-run equilibrium states $\mathbf{\Pi}(\boldsymbol{x}'_{\mathrm{t}-1}, \boldsymbol{w}'_{\mathrm{t}-1})'$.

If $\mathbf{\Pi}$ is set to zero (as some modellers do) the VAR model would only describe stationary changes of the climate variables, but such a model could not represent the more important long-run properties of climate data.

If the VAR model is specified in levels of variables (without transforming into differences and cointegrated relations) then the problem of nonstationarity (or near nonstationarity) discussed in Sect. 1 would invalidate the statistical inference and render measures such as R^2 useless.[1]

In contrast, the CVAR formulation preserves all long-run information in the data while at the same time guarantees the correct use of standard statistical tables (χ^2, F, t). As the endogenous variables in the CVAR are given as $\Delta \boldsymbol{x}_t$, the validity of R^2 is ensured. By replacing the concept of correlation with cointegration, the CVAR model can be used to evaluate whether climate variables are causally associated without the peril of spurious correlations.

[1] Also a correlation coefficient (defined in terms of deviations from a constant mean) is only appropriate for stationary variables but not for nonstationary variables. In the latter case it is generally meaningless and can be completely misleading (Granger and Newbold, 1974).

CPD
6, 2557–2591, 2010

Glacial cycles: drivers

R. K. Kaufmann and K. Juselius

Thus, the problem of pronounced time dependence typical of climate variables is likely to invalidate the estimates from many of the most commonly used regression models. We use the CVAR model as our statistical model is because it specifically designed to analyze nonstationary time series – ignoring this aspect of climate data can easily generate very misleading results.

2.5 A CVAR model for paleoclimate data

As the main purpose is to evaluate the role that orbital, seasonal, and spatial variations in solar insolation play in glacial cycles, we estimate CVAR models that differ according to the components of solar insolation included and evaluate the ability of these models to simulate glacial cycles of *Temp*, CO_2, and *Ice*. For example, one possible scenario postulates that solar variables alone explain these long-run movements in glacial cycles. Another scenario postulates that internal climate dynamics play a crucial role in the generation of glacial cycles. A third scenario postulates that glacial cycles are driven by both exogenous solar variables and internal climate dynamics.

In the first case, $\mathbf{\Pi}$ matrix would be full rank and equal to the number of endogenous variables. Each climate variable would cointegrate with some (or all) exogenous solar variables so that these cointegrating relations would define a unique equilibrium for each endogenous climate variable as a function of the exogenous variables. In the other two cases the $\mathbf{\Pi}$ matrix would have reduced rank, which suggests that the mechanisms underlying glacial cycles need to be explained both by exogenous solar variables and the internal climate dynamics. Regardless of which case is correct, the estimated $\hat{\mathbf{\Pi}}$ matrix can be used in the simulations as illustrated below.

Consider the first row of the $\mathbf{\Pi} z_{t-1}$ matrix where for illustrative purposes $z'_t = (\boldsymbol{x}'_t, \boldsymbol{w}_t)$ and $\boldsymbol{x}'_t = [\text{Temp}_t, \text{CO}_{2_t}, \text{Ice}_t]$ and $\boldsymbol{w}_t = \text{obliquity}_t$:

$$\boldsymbol{\pi}_1 z_t = \boldsymbol{\alpha}_{11} \boldsymbol{\beta}'_1 z_t + \boldsymbol{\alpha}_{12} \boldsymbol{\beta}'_2 z_t + \boldsymbol{\alpha}_{13} \boldsymbol{\beta}'_3 z_t$$

If $\mathbf{\Pi}$ has full rank then $\boldsymbol{\beta}'_i z_t \sim I(0)$, $i = 1, 2, 3$. Because a linear combination of stationary variables is also stationary, $\boldsymbol{\pi}_1 z_t$ is also stationary, i.e. $\boldsymbol{\pi}_1 z_t$ defines a stationary

CPD
6, 2557–2591, 2010
Glacial cycles: drivers
R. K. Kaufmann and K. Juselius

relation. If $\mathbf{\Pi}$ has reduced rank, say 2, then the third component, $\boldsymbol{\beta}'_3 z_t$, is nonstationary and $\boldsymbol{\alpha}_{13} = 0$. Also in this case $\boldsymbol{\pi}_1 z$ would define a stationary relation. If however $\boldsymbol{\beta}'_3 z_t$ is a near unit root process in the sense discussed above, then $\boldsymbol{\beta}'_3 z_t$ would exhibit a pronounced persistence and $\boldsymbol{\alpha}_{13}$, though close to zero, might nevertheless be significant. For example, assume that $\boldsymbol{\alpha}_{13} = 0.01$. If significant, it would correspond to an average adjustment time of $\ln(2)/0.01 = 70$ periods. Though not very important in the short run it would be very important for the long-term properties of the model. If not significant, it would just add noise to the simulations and, therefore, imply some small efficiency loss. This, however, would not in general be harmful to the simulation results.

As shown by Eq. (7), $\boldsymbol{\alpha}\boldsymbol{\beta}'\boldsymbol{x}_{t-1}$ is equal to $\mathbf{\Pi}\boldsymbol{x}_{t-1}$ and we can use either to investigate the feed-back properties of the system. For the purpose of this paper (to evaluate the role that exogenous orbital, seasonal, and spatial variations in solar insolation play in glacial cycles) there is no benefit of using $\boldsymbol{\alpha}\boldsymbol{\beta}'\boldsymbol{x}_{t-1}$ rather than $\mathbf{\Pi}\boldsymbol{x}_{t-1}$, and the simulations are, therefore, based on the latter. Because a cointegration relation that exhibits fairly pronounced persistence can have significant predictive power in simulations over the long run (while over the short run it does not add much explanatory power) the rank of the $\mathbf{\Pi}$ matrix conditional on the exogenous drivers has been liberally selected. This means that that the simulations are based on a CVAR model with a dynamic structure containing a characteristic root which is fairly close to, but not on the unit circle.

2.6 Experimental design

The fully parameterized CVAR model (Eq. 6) is used to generate in-sample simulations for each of three endogenous variables, *Temp*, CO_2, and *Ice*. Simulations are initialized with observed values prior to the start date (391 kyr before present). To identify the component(s) of solar insolation that determines the ability of the CVAR model to simulate glacial cycles, we estimate three basic models that vary according to the set of exogenous variables (Table 2). The three basic models are motivated by three basic hypotheses, which are given below:

CPD
6, 2557–2591, 2010

Hypothesis 1: Glacial cycles can be simulated by strong correlations among surface temperature, CO_2, and ice volume

To test this hypothesis, we specify Model 1, which includes three endogenous variables, *Temp*, CO_2, and *Ice*, and one exogenous variable, solar insolation as measured by annual solar insolation (*Insol*0) at 65° N. This variable is chosen because it is commonly used as a driver of glacial cycles (Kukla et al., 1981; Imbrie et al., 1993). If hypothesis 1 is correct, Model 1 should generate accurate in-sample simulations for *Temp*, CO_2, and *Ice*. Failure to generate accurate in-sample simulations indicates either that; (1) strong correlations among surface temperature atmospheric concentrations of carbon dioxide, and ice volume are not sufficient to simulate glacial cycles or (2) cumulative annual solar insolation at 65° N does not fully capture the role of solar insolation in glacial cycles.

Hypothesis 2: Some aspects of orbital, seasonal, and spatial variations in solar insolation play a more important role in glacial cycles than others

To test this hypothesis we create several versions of Model 2, each of which extends Model 1 (the control) by including one or more of the following groups of variables for solar insolation:

1. precession, obliquity, and eccentricity capture variations in solar insolation that are associated with changes in Earth's orbit,
2. solar insolation on 21 March (*SunSpr*), 21 June (*SunSum*), 21 September (*SunAut*), and 21 December (*SunWin*) at 65° N capture seasonal variations in solar insolation,
3. cumulative annual solar insolation at 65° N for days on which the diurnal average insolation intensity exceeds 275 W/m^2, (*Insol*275) and cumulative annual solar insolation for days on which intensity exceeds 550 W/m^2 (*Insol550*) at 65° N,

capture the effects of summer-time variations that are described by Huybers and Denton (2008).

Because results indicate that group 1 (precession, obliquity, and eccentricity) generates the most accurate in-sample simulations, and because there is an extensive literature on the role of each component, additional models examine the ability of precession, obliquity, and eccentricity to individually simulate glacial cycles.

Hypothesis 3: Solar insolation at 65° N is the best proxy for spatial and temporal specific effects of orbital changes in solar insolation

To test this hypothesis, the four time series of seasonal solar insolation and the three time series of cumulative annual solar insolation measured at 65° N in Model 2e are successively replaced by measurements from each of twelve latitudes spaced 5° apart from 60° to 85° North and South (Model 3). For example, one of the twelve versions of Model 3 specifies *SunSpr*, *SunSum*, *SunAut*, *SumWin*, *Insol0*, *Insol275*, and *Insol550* measured at 75° S.

Choosing the most accurate in-sample simulation

We test these hypotheses by comparing the accuracy of in-sample simulations generated by competing models. The ability of Models 1–3 to simulate *Temp*, CO_2, and *Ice* is assessed using the following loss function:

$$d_t = (x_t - \hat{x}_{i,\mathrm{t}})^2 - (x_t - \hat{x}_{j,\mathrm{t}})^2$$

where x_t is the observed value of endogenous variable x for period t, $\hat{x}_{\mathrm{s,t}}$, $s = i, j$, is the in-sample simulation for endogenous variable x simulated by model s for period t. Values of d_t are used to calculate the $S_{2\mathrm{a}}$ test statistic (Lehman, 1975) as follows:

$$S_{2\mathrm{a}} = \frac{\sum I_+(d_t) - 0.5\,N}{\sqrt{0.25\,N}}$$

CPD
6, 2557–2591, 2010
Glacial cycles: drivers
R. K. Kaufmann and K. Juselius

in which $I_{+}(d_t) = 1$ if $d_t > 0$, and 0 otherwise and N is the number of observations (391).

The S_{2a} statistic tests the null hypothesis that models i and j are able to simulate endogenous variable x with equal accuracy. Under this null hypothesis, the S_{2a} test statistic is asymptotically standard normal. A positive value for the S_{2a} statistic that exceeds the $p = .05$ threshold (1.96) indicates that the in-sample simulation for endogenous variable x generated by model j is closer to the observed value than the in-sample simulation for endogenous variable x generated by model i more often than expected by random chance and, hence that model j generates a more accurate in-sample simulation of variable x than model i.

Are results sensitive to a model's number of explanatory variables?

Reviewers of a previous version of this manuscript express concern that increasing the number of explanatory variables increases the explanatory power of a model by definition. The effect of adding more variables on the statistical significance of results is captured by the degrees of freedom, which measures the number of values in the final calculation of a statistic that are free to vary. Because the number of observations is large (391), the penalty for adding additional explanatory variables is small. For example, each equation in Model 1 (the model with the fewest explanatory variables) has 380 degrees of freedom. Model 2e, and all versions of Model 3 (the models with the greatest number of explanatory variables) have 353 degrees of freedom. This reduction in the degrees of freedom has a tiny effect on the critical value of the t distribution that is used to evaluate diagnostic statistics. For example, the significance level for a t statistic with a value of 2.0 and has 380 degrees of freedom is 0.0462, the significance level is 0.0463 for 353 degrees of freedom. Consistent with this small effect, increases in the number of explanatory variables do not automatically increase explanatory power. For example, Sect. 4 includes several comparisons in which increasing the number of explanatory variables in a model does not increase the accuracy of its in-sample simulation.

CPD
6, 2557–2591, 2010

Glacial cycles: drivers

R. K. Kaufmann and K. Juselius

3 Results

Are climate time series stationary or nonstationary? As can be seen from Figures 1a-c there is a pronounced persistence in the way *Temp*, CO_2, and *Ice* evolve over time. Such persistence suggests that the variable is nonstationary with $\rho = 1$ (a unit root process) or approximately so with ρ close to 1 (a near unit root process). For all models tested, the rank of the $\mathbf{\Pi}$ matrix seems less than full rank suggesting that solar variables alone cannot explain glacial cycles. For all models, the adjustment coefficients to the last cointegration relation are small in absolute size but borderline significant. As already discussed, this is an indication that the last cointegrating relation contains information which has a tiny short-run effect on the climate whereas potentially very important long-run effect on glacial cycles. Therefore, the $\mathbf{\Pi}$ matrix is assigned full rank, implying that the number of cointegrating relationships is set equal to the number of endogenous variables. We conclude that the endogenous climate variables are nonstationary (or very closely so) and that glacial cycles are driven by exogenous solar variables and internal climate dynamics.

For most comparisons (57/63), the S_{2a} statistic (Table 3) rejects ($p < 0.05$) the null hypothesis, which indicates that one model generates a more accurate in-sample simulation than another. The latitudinal set of exogenous variables for solar insolation that generates the most accurate simulation varies among the three endogenous variables (Table 4). The most accurate simulation for each of the endogenous variables is chosen from among the twelve simulations based on the number of "wins" relative to "losses". Wins are defined as a comparison in which the S_{2a} statistic identifies the simulation as more accurate ($p < .05$) – losses are defined as a comparison in which the S_{2a} statistic identifies the simulation as less accurate ($p < .05$).

Using this criterion, there is fairly strong evidence for a "most accurate simulation" for surface temperature and ice volume (Table 4). Surface temperature is simulated most accurately (nine wins, no losses) by a version of Model 3 that measures solar insolation at 75° N. Conversely, ice volume is simulated most accurately (nine wins, no

CPD
6, 2557–2591, 2010

losses) by a version of Model 3 that measures solar insolation at 60° S. The twelve versions of Model 3 differ little in their ability to simulate atmospheric concentrations of carbon dioxide. There are only fifteen comparison in which one version of Model 3 generates a more accurate (less accurate) simulation, compared to thirty three for surface temperature and thirty nine for ice volume. Of these fifteen definitive comparisons, there is some indication that insolation in the Southern Hemisphere generates the most accurate in-sample simulations for CO_2, as indicated by models that measure solar insolation at 65° S (three wins no losses) and 70° S (four wins, no losses).

4 Discussion

4.1 Testing H1: Strong statistical associations among endogenous variables temperature, CO_2, and ice volume are sufficient to explain glacial cycles

As suggested by (Fig. 1a–c), Model 1 is not able to reproduce the large fluctuations in *Temp*, CO_2, and *Ice* in a meaningful fashion. For example, the in-sample simulation generated by Model 1 is able to account for only 21% of the observed variation in temperature.

This inability may seem surprising given that previous analyses indicate that strong statistical associations exist among *Temp*, CO_2, and *Ice*. But, because R^2 measures a model's fit of an endogenous variable given the *observed* values of the other variables, it need not be a good measure of a model's ability to simulate glacial cycles. To illustrate, we use Model 1a to simulate temperature and ice endogenously assuming that CO_2 (along with annual solar insolation at 65° N) is given exogenously, i.e. endogenously simulated values of CO_2 are replaced with observed values for CO_2, which allows *Temp* and *Ice* to adjust towards equilibrium values implied by the observed values of CO_2.

This change in model specification increases the ability of Model 1a to simulate values for temperature (Fig. 1a). Measured by the R^2 of the in-sample forecast, Model

CPD
6, 2557–2591, 2010

Glacial cycles: drivers

R. K. Kaufmann and K. Juselius

1a can account for 64% of the variation in temperature. This, however, is still less than the R^2 between observed values of CO_2 and temperature, which is 0.77.

The inability of Model 1 to reconstruct glacial cycles accurately based on the very strong correlations among *Temp*, CO_2, and *Ice*, highlights the power of the CVAR model and the importance of exogenous drivers of the climate system. If the CVAR model is based simply on correlations, the strong correlations among *Temp*, CO_2, and *Ice*, would allow Model 1 to simulate glacial cycles accurately. That Model 1a cannot simulate glacial cycles accurately even when given the historical observations for CO_2 suggests that the correlations among surface temperature, CO_2, and ice volume are driven by some other factor, either a component of solar insolation not included in Model 1 (Sect. 3.2) or a component of the climate system that is not included in Model 1.

4.2 Testing H2: Orbital, seasonal, and spatial variations in solar insolation are particularly important for glacial cycles

The inability Model 1 to reproduce the glacial cycles may be sensitive to the variable used to represent solar insolation, *Insol0*. For example, Milankovitch and others argue that mid-summer insolation at 65° N is critical because that is the season and latitude where ice sheets wax and wane. To test the importance of orbital and seasonal variations in solar insolation, we estimate Models 2a–c that contain variables for solar insolation from one of three groups: (1) Model 2a orbital changes (precession, obliquity, eccentricity); (2) Model 2b seasonal variations (*SunSpr, SunSum, SunAut* and *SunWin*) and; (3) Model 2c variations in cumulative summer insolation (*Insol*275 and *Insol*550).

Figures 2a–c suggest that including orbital or seasonal variations in solar insolation enhance the ability of Model 2a and Model 2b to simulate glacial cycles relative to Model 1. This result is confirmed by values of the S_{2a} statistic, which indicate the in-sample simulations of *Temp*, CO_2, and *Ice* generated by Model 2a and Model 2b are more accurate than the simulations generated by Model 1 (Table 3). Of these, Model 2a generates more accurate in-sample simulations than Model 2b.

To evaluate the explanatory power of seasonal variations (e.g. the Milankovitch forcing) relative to orbital variations, we estimate Model 2d, which adds the seasonal measures of solar insolation to Model 2a. The results indicate that Model 2d generates a more accurate ($p < .05$) simulation of CO_2 ($S_{2a} = 3.44$, $p < .001$) and *Ice* ($S_{2a} = 2.33$, $p < 0.021$). Conversely, the in-sample temperature simulation generated by Model 2d is not statistically different from that generated by Model 2a ($S_{2a} = 0.81$, $p > 0.41$). Together, these results indicate that seasonal variations in solar insolation at 65° N have explanatory power about glacial cycles that extend beyond aggregate measures of orbital variations.

Conversely, the simulations generated by Model 2c are not more accurate than those generated by Model 1 (Table 3). Similarly, adding *Insol*275 and *Insol*550 to Model 2d (to create Model 2e) does not increase the accuracy of the in-sample simulation for *Temp* ($S_{2a} = 1.32$, $p > 0.18$) and CO_2 ($S_{2a} = 1.11$, $p > 0.26$). For *Ice* the in-sample forecast generated by Model 2e is less accurate than the in-sample forecast generated by Model 2d ($S_{2a} = 6.18$, $p < 0.001$). Together, these results indicate that simply adding more variables to the CVAR does not improve its performance and that *Insol*275 and *Insol*550 have little explanatory power relative to orbital and seasonal variations in solar insolation. The latter can be interpreted at least three ways; (1) cumulative summer solar insolation is unimportant, (2) the effect of cumulated summer insolation is subsumed by orbital or seasonal measures of solar insolation, or (3) the effect of cumulative summer-time insolation occurs at a latitude other than 65° N (Sect. 4.4).

4.3 Further tests of H2: Obliquity paces late Pleistocene terminations

Continuing with the logic from the previous section, it has been argued that some components of orbital changes are more important to glacial cycles than others. To test the null hypothesis that glacial terminations are independent of precession, obliquity, or eccentricity, Huybers and Wunsch (2005) analyze the leading empirical orthogonal

CPD
6, 2557–2591, 2010
Glacial cycles: drivers
R. K. Kaufmann and K. Juselius

function of ten well-resolved marine $\delta^{18}O$ records. Results reject the null hypothesis that glacial terminations are independent of obliquity at the five percent significance level. Conversely, this hypothesis cannot be rejected for eccentricity or precession, which implies that obliquity alone paces late Pleistocene terminations.

We evaluate these results by estimating versions of Model 2 that include either: obliquity (Model 2f), eccentricity (Model 2g), or precession (Model 2h). None of the three models simulates changes in *Temp*, CO_2, and *Ice* in a way that can be considered a meaningful representation of glacial cycles (Fig. 3a–c). Of the three, Model 2g, the model that includes precession, generates the most accurate in-sample simulations (Table 3), but only because its small amplitude keeps it closer to the simple mean values for temperature, CO_2, and ice volume. Conversely, Model 2f, simulates large changes that can be interpreted as glacial and interglacial periods.

But obliquity is not a sufficient explanatory variable for glacial terminations. As indicated in Fig. 3a–c, Model 2f simulates several false terminations, which we define as large reductions in ice cover (and increases in temperature and atmospheric CO_2) that are not present in the observational record. For example, Model 2f simulates a large reduction in ice volume about 90 kyr before the present (Fig. 3c), but there is no noticeable reduction in the observational record.

Huybers and Wunsch (2005) recognize this difficulty and suggest that the climate state skips one or two obliquity beats before deglaciating. By way of explanation, they suggest that high latitude insolation and thickness of the ice sheet determine whether a glacial termination event occurs. This explanation seems unlikely. Replacing annual solar insolation at 65° N with corresponding values at latitudes between 60° and 85° from the Northern or Southern Hemisphere does not allow a modified version of Model 2f to improve its ability to differentiate obliquity cycles that do and do not generate deglaciations. The thickness of ice may determine whether an obliquity cycle generates a deglaciation event, but Model 2f is not able to simulate ice volume with sufficient accuracy to do so.

CPD
6, 2557–2591, 2010

R. K. Kaufmann and K. Juselius

Conversely, Model 2a, which contains precession and eccentricity in addition to obliquity, generally is able to translate obliquity cycles into glacial terminations (Fig. 2a–c). This capability suggests that eccentricity and precession influence, either directly or indirectly via other endogenous climate variables (e.g. ice thickness), whether changes in obliquity generate a glacial termination. As such, these results contradict the findings by Huybers and Wunsch (2005) that glacial terminations are independent of eccentricity and precession.

4.4 Testing H3: solar insolation in the Northern Hemisphere drives glacial cycles

The results reported in Table 4 indicate that glacial cycles in *Ice* and maybe CO_2 are best simulated by solar insolation in the Southern Hemisphere. Although there is no clear best simulation for CO_2, in general, the better simulations are generated by models that measure solar insolation in the Southern Hemisphere. This relation can be explained in terms of recent hypotheses about the role of ocean circulation. According to these hypotheses, ice cover (Stephens and Keeling, 2000) and ocean overturning (Francois et al., 1997; Toggweiler, 1997; Watson and Garabato, 2006) in the high latitudes of the Southern Ocean drive atmopspheric CO_2 concentrations that influence glacial cycles. Similarly, results that indicate solar insolation in the Northern Hemisphere is most strongly related to surface temperature are consistent with hypotheses about the role of North Atlantic deep water in glacial cycles (Imbrie et al., 1993; Gildor and Tziperman, 2001). Finally, that solar insolation in the Southern Hemisphere generates the most accurate simulations for ice volume is consistent with findings by (Petit et al., 1999) and results that indicate driving a single column atmosphere model with cumulative summer insolation in the Southern Hemisphere generates the most accurate simulation of ice volume at Dome F (Huybers and Denton, 2008).

Conversely, our results contradict statistical results and mechanistic explanations for the relations between hemispheric insolation and surface temperature and/or ice

CPD
6, 2557–2591, 2010

volume. For example, Huybers and Denton (2008) argue that insolation in the Southern Hemisphere summer is the more important driver of temperature in the Antarctic.

5 Conclusions

Although the statistical models for glacial cycles reported here cannot replace models based on physical mechanisms, a CVAR can be used to test competing hypotheses against the observational record. Here, we demonstrate that a CVAR can simulate much of the variation in *Temp*, CO_2, and *Ice* that is associated with glacial cycles. To do so, the CVAR must include a suite of variables for solar insolation that represent changes in Earth's orbit and seasonal variations at various latitudes. Solar insolation in the Southern Hemisphere generates the most accurate in-sample simulations for ice volume and maybe atmospheric CO_2 while solar insolation in the Northern Hemisphere generates the most accurate in-sample simulation for surface temperature.

The ability of the CVAR to identify the drivers of glacial cycles extends well beyond previous efforts. Statistical relationships among time series in the CVAR model are not spurious. The presence of cointegrating relationships indicates that time series share the same stochastic trend, which implies that time series have a long-run relationship. These long-run relationships and the dynamics by which variables adjust to disequilibrium are embodied in the $\mathbf{\Pi}$ matrix of Eq. (2).

In this first step of an on-going research effort organized around a CVAR model, we do not disentangle long- and short-run relationships. Future research will add endogenous variables that may connect solar insolation to surface temperature, atmospheric CO_2, or ice volume and/or may proxy the physical mechanisms that connect these three endogenous variables. To test hypotheses about these linkages, the $\mathbf{\Pi}$ matrix of this expanded CVAR model will be decomposed by imposing over-identifying restrictions. Identifying the CVAR will allow us to explore the following topics:

CPD
6, 2557–2591, 2010

- Quantify the long-term temperature sensitivity to a doubling of atmospheric CO_2 (ΔT_{2x}). The identified CVAR also will allow us to separate the direct effect from the full ice-albedo feedback.
- Quantify the dynamics by which changes in solar insolation affect endogenous variables and the mechanisms by which these effects are transmitted through the climate system. This will build on current efforts that seek to match turning points in time series (Caillon et al., 2003).
- Test hypotheses about the mechanisms that drive changes in the endogenous variables. For example, testing whether iron dust, sea-surface temperature, and/or non sea salt sodium are part of the cointegrating relationship for CO_2 will allow us to test whether iron fertilization, ocean overturning, and/or ice cover, respectively, play an important role in controlling atmospheric CO_2 during glacial cycles (Sigman and Boyle, 2000).
- Test the hypothesis that the nature of glacial cycles changes over time. For most of the endogenous variables, data are available over the last 750 kyr. We will estimate the CVAR over this full period and test whether the long-term relationships and/or rates of adjustment change in a statistically meaningful way. We will also use the model to "backcast" the endogenous variables and compare the simulated values for ice volume over the last several million years, for which data are available.
- Test the "Ruddiman hypothesis" that anthropogenic climate change starts about 5000 years ago. We will include times series for atmospheric CO_2 and CH_4 emissions associated with anthropogenic activities as exogenous variables and test whether anthropogenic emissions improve the model's ability to simulate the last glacial termination, which it currently does poorly.

CPD
6, 2557–2591, 2010

We do not expect any one of these analyses to be definitive. But they will add to on-going investigations by using rigorous statistical techniques to test what is and is not consistent with the observational record.

References

Adhemar, J.: Revolutions de la Mer: Deluges periodiques, Carillian-Geeury et V. Dalmont, Paris, 1842. 2558

Bender, M.: Climate-biosphere interactions on glacial-interglacial timescales, Global Biogeoch. Cy., 17, 1–10, 2003. 2559

Caillon, N., Severinghaus, J. P., Jouzel, J., Barnola, J.-M., Kang, J., and Lipenkov, V. Y.: Timing of Atmospheric CO_2 and Antarctic Temperature Changes Across Termination III, Science, 299, 1728–1731, 2003. 2580

Croll, J.: Climate and Times in Their Geological Relations: a Theory of Secular Changes in the Earth's Climate, Appleton, New York, 1875. 2558

Francois, R., Altabet, M., Yu, E., Sigman, D., Bacon, M. P., Frank, M., Bohrmann, G., Bareille, G., and Labeyrie, L.: Contribution of Southern Ocean surface-water stratification to low atmospheric CO_2 concentrations during the last glacial period, Nature, 389, 929–935, 1997. 2578

Gildor, H. and Tziperman, E.: Physical mechanisms behind biogeochemical glacial-interglacial CO_2 variations, Geophys. Res. Lett., 28, 2421–2424, 2001. 2578

Hays, J.: Antarctic Glacial History and World Paleoenvironments, New York Times, 57–71, 1978. 2560

Hays, J., Imbrie, J., and Shackleton, J.: Variations in the Earth's orbit: pacemaker of the ice ages, Science, 194, 1121–1132, 1976. 2558

Hendry, D. and Juselius, K.: Explaining coinegration analysis: Part 1, Energy Journal, 21, 1, 2000. 2565

Huybers, P. and Denton, G.: Antarctic temperature at orbital timescales controlled by local summer duration, Nat. Geosci., 1(11), 787–792, 2008. 2560, 2578, 2579, 2585

Imbrie, J., Berger, A., Boyle, E., Clemens, S., Duffy, A., Howard, W., Kukla, G., Kutzbach, J., Martinson, D., Mcintyre, A., Mix, A., Molfino, B., Morley, J., Peterson, L., Pisias, N., Prell, W., Raymo, M., Shackleton, N., and Toggweiler, J.: On the structure and origin of major

CPD
6, 2557–2591, 2010
Glacial cycles: drivers
R. K. Kaufmann and K. Juselius

glaciation cycles 2 The 100,000-year cycle, Paleoceanography, 8, 699–735, 1993. 2559, 2560, 2570, 2578

Jouzel, J., Masson-Delmotte, V., Cattani, O., Dreyfus, G., Falourd, S., Hoffmann, G., Minster, B., Nouet, J., Barnola, J. M., Chappellaz, J., Fischer, H., Gallet, J. C., Johnsen, S., Leuenberger, M., Loulergue, L., Luethi, D., Oerter, H., Parrenin, F., Raisbeck, G., Raynaud, D., Schilt, A., Schwander, J., Selmo, E., Souchez, R., Spahni, R., Stauffer, B., Steffensen, J. P., Stenni, B., Stocker, T., Tison, J. L., Werner, M., and Wolff, E.: Orbital and millennial Antarctic climate variability in Antarctic climate variability over the past 800,000 years, Science, 317, 793–796, 2007. 2560, 2585

Kawamura, K., Parrenin, F., Lisiecki, L., Uemura, R., Vimeux, F., Severinghaus, J. P., Hutterli, M. A., Nakzawa, T., Aoki, S., Jouzel, J., Raymo, M. E., Matsumoto, K., Nakata, H., Motoyama, H., Fujita, S., Goto-Azuma, K., Fujii, Y., and Watanabe, O.: Northern Hemisphere forcing of climatic cycles in Antarctica over the past 360,000 years, Nature, 448, 912–917, 2007. 2560

Kukla, G., Berger, R., and Brown, J.: Orbital signature of interglacials, Nature, 290, 295–300, 1981. 2570

Lehman, E.: Nonparametrics; Statistical Methods Based on Ranks, McGraw-Hill, San Francisco, 1975. 2571

Lisiecki, L. E. and Raymo, M. E.: A Pliocene-Pleistocene stack of 57 globally distributed benthic $\Delta^{18}O$ records, Paleoceanography, 20, 1–17, 2005. 2585

Lorius, C., Jouzel, J., Ritz, C., Merlivat, L., Barkov, N., Korotkevich, Y., and Kotlyakov, V.: A 150,000-year climactic record from Antarctic ice, Nature, 316, 591–596, 1999. 2560

Luthe, D., Floch, M. L., Bereiter, B., Blunier, T., Blunier, J.-M., Barnola, J.-M., Siegenthaler, U., Raynaud, D., Jouzel, J., Fischer, H., Kawamura, K., and Stocker, T. F.: High-resolution carbon dioxide concentration record 650,000–800,000 years before present, Nature, 453, 379–382, 2008. 2559

Martinez-Garcia, A., Rosell-Mele, A., Geibert, W., Gersonde, R., Masque, P., Gaspari, V., and Barbante, C.: Links between iron supply, marine productivity, sea surface temperature, and CO_2 over the last 1 Ma, Paleoceanography, 24, 1–14, 2009. 2559

Masson, V., Vimeux, F., Jouzel, J., Morgan, V., Delmotte, M., Ciais, P., Hammer, C., Johnsen, S., Lipenkov, V. Y., Mosley-Thompson, E., Petit, J. R., Steig, E. J., Stievenard, M., and Vaikmae, R.: Holocene climate variability in Antarctica based on 11 ice-core isotopic records, Quarternary Res., 54, 348–358, 2000. 2560

Masson-Delmotte, V., Kageyama, M., Braconnot, P., Charbit, S., Krinner, G., C Ritz, E. G., Jouzel, J., Abe-Ouchi, A., Cruci, M., Gladstone, R., Hewitt, C., Kitoh, A., LeGrande, A., Marti, O., abd TMR Ohgaito, U. M., Otto-Bliesner, B., Peltier, W., Ross, I., Valdes, P., Vettorretti, G., Weber, S., Wolk, F., and Yu, Y.: Past and future polar amplification of climate change: climate model intercomparisons and ice-core constraints, Clim. Dynam., 26, 513–529, 2006. 2561

Masson-Delmotte, V., Stenni, B., Pol, K., Braconnot, P., Cattani, O., Falourd, S., Jouzel, J., Landais, A., Minister, B., Barnola, J., Chappellaz, J., Kinner, G., Johnsen, S., Rothlisberger, R., Hansen, J., Mikolajewicz, U., and Otto-Bliesner, B.: EPICA Dome C record of glacial and interglacial intensities, Quaternary Sci. Rev., 29, 113–128, 2010. 2561

Milankovitch, M.: Kanon der erdbestrahlung und seine andwendung auf das eiszeitenproblem, Serbian Acad. Spec. Publ., 132(33), 633, 1941. 2558

Muller, R. and MacDonald, G.: Spectrum of 100-kyr glacial cycle: Orbital inclination, not eccentricity, P. Natl. Acad. Sci. USA, 94, 8329–8334, 1997. 2559

Paillard, D.: Glacial Cycles: Toward a New Paradigm, American Geophysical Union, 39, 325–346, 2001. 2558, 2559

Paillard, D., Labeyrie, L., and Yiou, P.: Macintosh program performs time-series analysis, Eos Trans. AGU, 77, 379, 1996. 2585

Parrenin, F., Barnola, J.-M., Beer, J., Blunier, T., Castellano, E., Chappellaz, J., Dreyfus, G., Fischer, H., Fujita, S., Jouzel, J., Kawamura, K., Lemieux-Dudon, B., Loulergue, L., Masson-Delmotte, V., Narcisi, B., Petit, J.-R., Raisbeck, G., Raynaud, D., Ruth, U., Schwander, J., Severi, M., Spahni, R., Steffensen, J. P., Svensson, A., Udisti, R., Waelbroeck, C., and Wolff, E.: The EDC3 chronology for the EPICA Dome C ice core, Clim. Past, 3, 485–497, doi:10.5194/cp-3-485-2007, 2007. 2562

Petit, J. R., Jouzel, J., Raynaud, D., Barkov, N. I., Barnola, J.-M., Basile, I., Benders, M., Chappellaz, J., Davis, M., Delaygue, G., Delmotte, M., Kotlyakov, V., Legrand, M., Lipenkov, V., Lorius, C., Pepin, L., Ritz, C., Saltzman, E., and Stievenard, M.: Climate and atmospheric history of the past 420,000 years from the Vostok ice core, Antarctica, Nature, 399, 429–436, 1999. 2559, 2560, 2578

Raymo, M.: The timing of major climate terminations, Nature, 12, 577–585, 1997. 2560

Ruddiman, W. and Raymo, M.: A methane-based time scale for Vostok, Quarternary Sci. Rev., 22, 141–155, 2003. 2562

Saltzman, B. and Maasch, K.: A 1ST-Order global-model of late cenozoic climatic-change, T. Roy. Soc. Edinburch-Earth Sci., 81, 315–325, 1990. 2559

Schackleton, N. and Opdyke, N.: Oxygen isotope and paleomagnetic stratigraphy of equatorial Pacific core V28–238: oxygen isotope temperatures and ice volumes on a 105 and 106 scale, Quarternary Res., 3, 39–55, 1973. 2558

Shackleton, N. J.: The 100,000-Year Ice-Age Cycle Identified and Found to Lag Temperature, Carbon Dioxide and Orbital Eccentricity, Science, 289, 1897–1902, 2000. 2559

Siegenthaler, U., Stocker, T. F., Monnin, E., Lüthi, D., Schwander, J., Stauffer, B., Raynaud, D., Barnola, J.-M., Fischer, H., Masson-Delmotte, V., and Jouzel, J.: Stable Carbon Cycle-Climate Relationship During the Late Pleistocene, Science, 310, 1313–1317, 2005. 2559

Sigman, D. M. and Boyle, E. A.: Glacial/interglacial variations in atmospheric carbon dioxide, Nature, 407, 859–869, 2000. 2580

Stephens, B. and Keeling, R.: The influence of Antarctic sea ice on glacial-interglacial CO_2 variations, Nature, 404, 171–174, 2000. 2578

Toggweiler, J.: Variation of atmospheric CO_2 by ventilation of the oceans deepest water, Paleoceanography, 14, 571–588, 1997. 2578

Watson, A. and Garabato, A.: The role of SOuthern Ocean mixing and upwelling in glacial-interglacial atmospheric CO_2 change, Tellus B, 57, 73–87, 2006. 2578

Wolff, E., Fischer, H., Fundel, F., Ruth, U., Tawarloh, B., Littot, G., Mulvaney, R., Rothlisberger, R., de Angelis, M., Boutron, C., Hansson, M., Jonsell, U., Hutterli, M., Lambert, F., Kaufmann, P., Stauffer, B., Stocker, T. F., Steffensen, J., Bigler, M., Siggaard-Andersen, M., Udisti, R., Becagli, S., Castellano, E., Severi, M., Wagenbach, D., Barbante, C., Gabrielli, P., and Gaspari, V.: Southern Ocean sea-ice extent, productivity and iron flux over the past eight glacial cycles, Nature, 440, 491–496, 2006. 2559

Table 1. Time seres included in the CVAR.

Variable	Source	Unit	Time Scale	Obs
Temp	Jouzel et al. (2007)	Δavg. last 1 kyr	EDC3	710
CO_2	Lüthi et al. 2008	ppmv	ECD3	517
Ice	Lisiecki and Raymo (2005)	$\delta^{18}O$ (per mil)	LR04	390
Eccentricity	Paillard et al. (1996)	Dimensionless index	–	391
Obliquity	Paillard et al. (1996)	Degrees	–	391
Precession	Paillard et al. (1996)	Dimensionless index	–	391
Seasonal Insolation	Paillard et al. (1996)	W/m^2	–	391
Cumulative Summer Insol	Huybers and Denton (2008)	Giga Joules	–	391

CPD
6, 2557–2591, 2010

Glacial cycles: drivers

R. K. Kaufmann and K. Juselius

Table 2. Specification of the estimated CVARs.

	Endogenous	Exogenous Variables
Model 1	T, CO_2, Ice	Insol0,
Model 1(a)	T, Ice	CO_2, Insol0,
Model 1(b)	T, CO_2, Ice	SunSum,
Model 2a	T, CO_2, Ice	Insol0, Obl, Prec, Ecc
Model 2b	T, CO_2, Ice	Insol0, SunSpr, SunSum, SunFall, SunWin
Model 2c	T, CO_2, Ice	Insol0, Insol275, Insol550
Model 2d	T, CO_2, Ice	Insol0,Obl, Prec, Ecc, SunSpr, SunSum, SunFall, SunWin
Model 2e	T, CO_2, Ice	Obl, Prec, Ecc, SunSpr, SunSum, SunFall, SunWin, Insol0, Insol275, Insol550
Model 2f	T, CO_2, Ice	Insol0, Obl
Model 2g	T, CO_2, Ice	Insol0, Prec
Model 2h	T, CO_2, Ice	Insol0, Ecc
Model 3	T, CO_2, Ice	Obl, Prec, Ecc, SunSpr, SunSum, SunFall, SunWin, Insol0, Insol275, Insol550

CPD
6, 2557–2591, 2010

Glacial cycles: drivers

R. K. Kaufmann and K. Juselius

Table 3. In-sample accuracy of Model 2a–Model 2g as indicated by the S_{2a} statistic.

	Model j					
	Model 2a	Model 2b	Model 2c	Model 2f	Model 2g	Model 2h
Model i						
Temperature Comparison.						
Model 1	5.87**	6.58**	1.42	−8.51**	−1.52	−10.13**
Model 2a		−2.03*	−5.67**	−11.34**	−6.99**	−11.54**
Model 2b			−7.80**	−10.43**	−8.00**	−10.53**
Model 2c				−7.09**	−3.04**	−10.13**
Model 2f					8.10**	0.20
Model 2g						−10.23**
CO_2 Comparison						
Model 1	7.09**	6.38**	1.11	−11.14**	−3.24**	−9.52**
Model 2a		−1.82+	−5.47**	−11.57**	−7.49**	−10.03**
Model 2b			−6.07**	−12.46**	−6.48**	−9.82**
Model 2c				−11.34**	−3.85**	−9.62**
Model 2f					11.34**	7.39**
Model 2g						−10.23**
Ice Comparison						
Model 1	9.52**	7.80**	1.01	−14.28**	−4.66**	−12.66**
Model 2a		−3.33*	−7.19**	−16.61**	−9.92**	−15.70**
Model 2b			−7.49**	−16.20**	−9.32**	−14.79**
Model 2c				−13.87**	−6.48**	−13.87**
Model 2f					15.39**	7.19**
Model 2g						−14.48**

CPD
6, 2557–2591, 2010

Table 4. Summary statistics of the 12 × 11 comparison for in-sample accuracy as generated by the S_{2a} statistics for each of the three endogenous variables.

	Temp Wins	Losses	CO_2 Wins	Losses	Ice Wins	Losses
North 60	1	1	0	2	1	5
North 65	0	5	1	2	1	4
North 70	0	7	0	5	0	11
North 75	9	0	1	0	1	2
North 80	1	3	0	3	1	6
North 85	3	1	0	1	4	1
South 60	4	2	1	1	10	0
South 65	2	4	3	0	6	0
South 70	6	1	5	0	5	1
South 75	0	7	0	2	1	6
South 80	6	0	3	0	5	1
South 85	2	3	3	1	5	3

CPD
6, 2557–2591, 2010

Glacial cycles: drivers

R. K. Kaufmann and K. Juselius

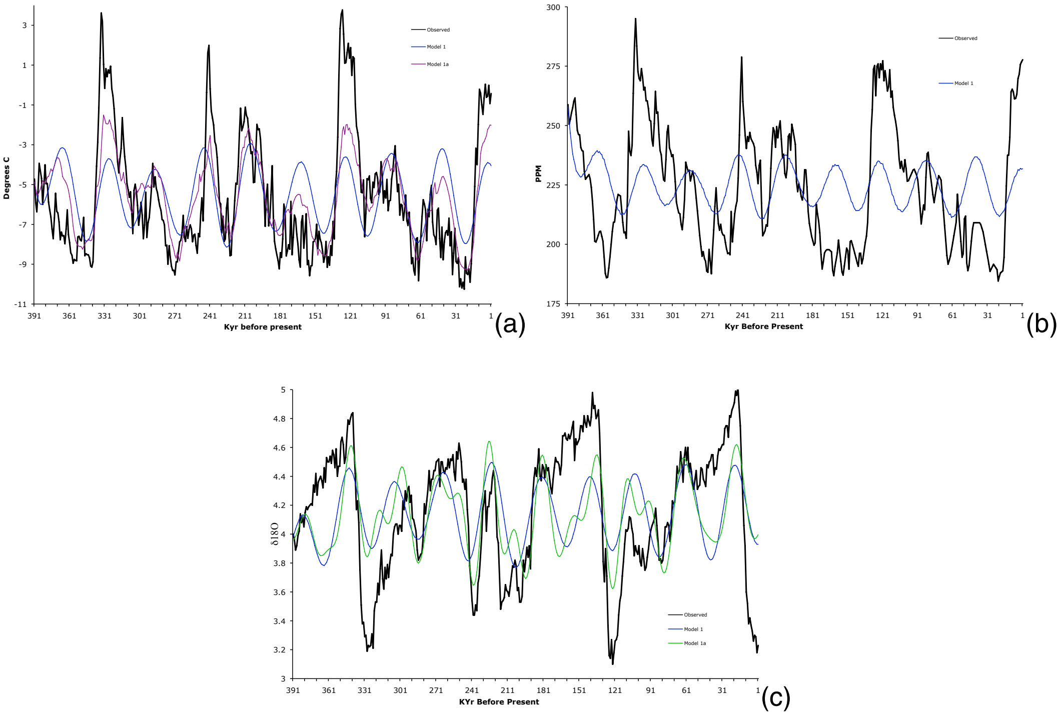

Fig. 1. **(a)** Observed values of temperature and values simulated by various versions of Model 1. **(b)** Observed values of atmospheric CO_2 and values simulated by various versions of Model 1. **(c)** Observed values of ice volume (as proxied by $\delta^{18}O$) and values simulated by various versions of Model 1.

CPD
6, 2557–2591, 2010

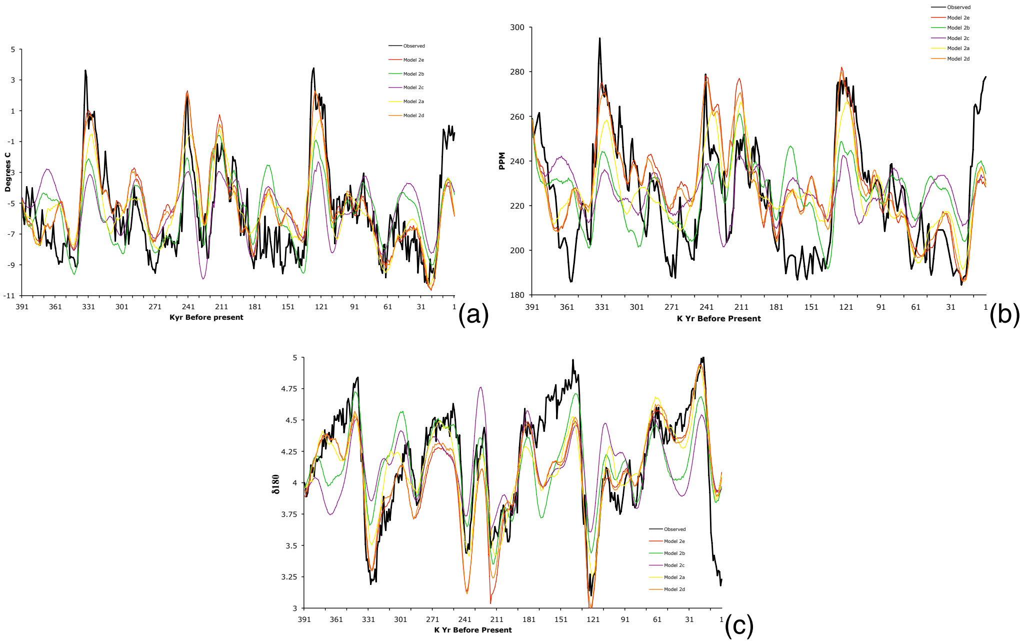

Fig. 2. **(a)** Observed values of temperature and values simulated by various versions of Model 2. **(b)** Observed values of atmospheric CO_2 and values simulated by various versions of Model 2. **(c)** Observed values of ice volume (as proxied by $\delta^{18}O$) and values simulated by various versions of Model 2.

CPD
6, 2557–2591, 2010

R. K. Kaufmann and K. Juselius

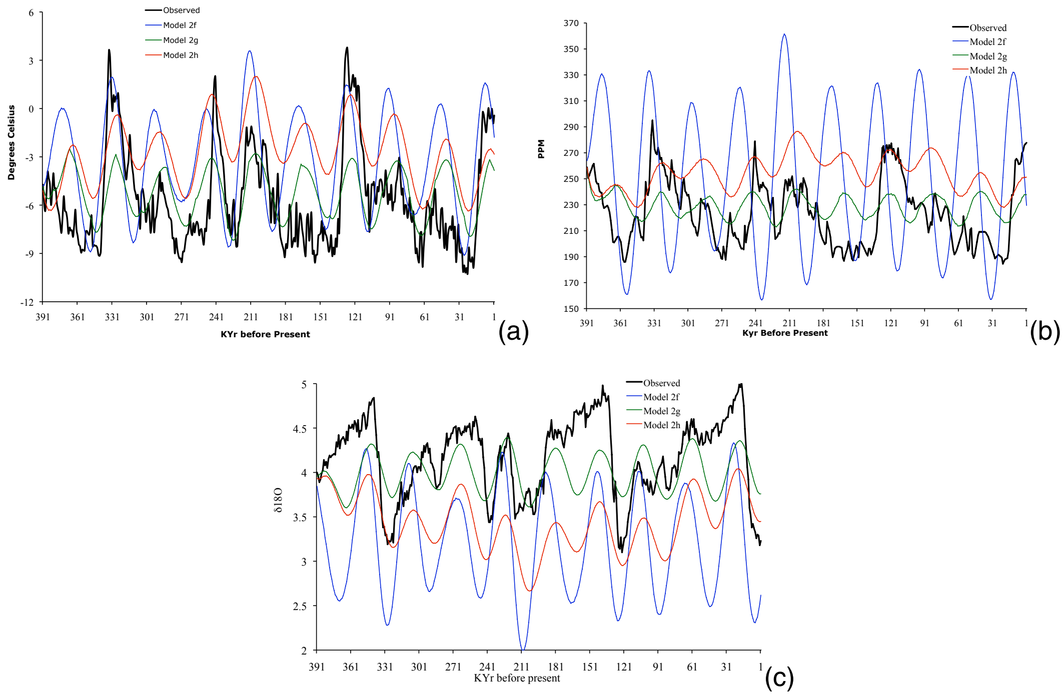

Fig. 3. **(a)** Observed values of temperature and values simulated by Model 2f–h. **(b)** Observed values of atmospheric CO_2 and values simulated by Model 2f–h. **(c)** Observed values of ice volume (as proxied by $\delta^{18}O$) and values simulated by Model 2f–h.

CPD
6, 2557–2591, 2010

Title Page
Abstract | Introduction
Conclusions | References
Tables | Figures
◀I | ▶I
◀ | ▶
Back | Close
Full Screen / Esc
Printer-friendly Version
Interactive Discussion